ChemPubSoc Europe

DOI: 10.1002/cbic.201500686

CHEMBIOCHEM Full Papers

SPECIAL ISSUE

Programmable DNA Hydrogels Assembled from Multidomain DNA Strands

Huiling Jiang,[a] Victor Pan,[a] Skanda Vivek,[b] Eric R. Weeks,[b] and Yonggang Ke*[a]

Hydrogels are important in biological and medical applications, such as drug delivery and tissue engineering. DNA hydrogels have attracted significant attention due to the programmability and biocompatibility of the material. We developed a series of low-cost one-strand DNA hydrogels self-assembled from single-stranded DNA monomers containing multiple palindromic domains. This new hydrogel design is simple and programmable. Thermal stability, mechanical properties, and loading capacity of these one-strand DNA hydrogels can be readily regulated by simply adjusting the DNA domains.

Introduction

Hydrogels, formed by crosslinking molecules in aqueous solution, have attracted considerable attention as important biomedical materials because of their desired properties, such as high water content, porosity, and tissue-like mechanics.[1] For example, hydrogels have been applied as three-dimensional carriers of mesenchymal stem cells due to their excellent biocompatibility and ability to retain large amounts of water.[2] Another important and widely explored application of hydrogels is drug delivery,[3] in which drugs can be incorporated into the interspace through chemical attachment or physical entrapment and subsequently released following various release stimuli, depending on the hydrogel properties. Both covalent and non-covalent interactions have been implemented for drug incorporation. Generally, multistep reactions are necessary for covalent functionalization, which are stable and irreversible.[4] Meanwhile, reversible non-covalent interactions such as hydrogen bonding, ionic interactions, and hydrophobic interactions have also been applied to load organic small drug molecules or inorganic nanoparticles into hydrogel systems.[5]

DNA has emerged as a important programmable material for biomaterial engineering.[6] In DNA hydrogels formed by Watson–Crick base pairing, researchers have realized a variety of desirable properties, such as self-healing, mechanical stability, minimal toxicity, and excellent biocompatibility.[7] However, previously reported DNA hydrogels typically utilize multistrand designs, are relatively expensive, and often require labor-intensive multistep syntheses.[5,8]

Here we report a low-cost one-strand DNA hydrogel design. We show that this simple system offers excellent programmability, in which mechanical properties and cargo loading capacity can be easily tuned by changing the strand sequences and lengths. We expect this new DNA hydrogel system will provide a new enabling platform for hydrogel-based biomedical applications.

Results and Discussion

The formulation of multistrand DNA hydrogel design typically involves two steps. First, structurally well-defined motifs assemble from multiple DNA strands. Then, the hydrogel is formed by joining the motifs together by base pairing. Our one-strand (OS) hydrogels use a different design strategy (Scheme 1). A DNA strand is designed to contain multiple domains, indicated by different colors. Each domain contains a self-complementary palindromic sequence. Hydrogel formation is a single-step

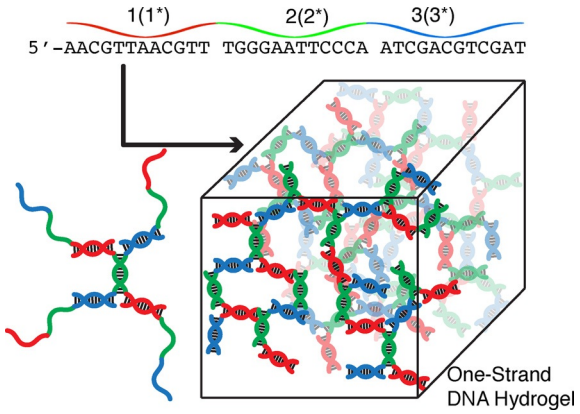

Scheme 1. One-strand (OS) multidomain DNA hydrogel. An OS strand consists of multiple domains, each containing a self-complementary palindromic sequence.

[a] *Dr. H. Jiang, V. Pan, Prof. Y. Ke*
Wallace H. Coulter Department of Biomedical Engineering
Emory School of Medicine
1760 Haygood Drive, Atlanta, Georgia 30322 (USA)
E-mail: yonggang.ke@emory.edu

[b] *S. Vivek, Prof. E. R. Weeks*
Emory University, Department of Physics
400 Dowman Drive, Atlanta GA 30322-2430 (USA)

Supporting information and the ORCID identification number(s) for the author(s) of this article can be found under http://dx.doi.org/10.1002/cbic.201500686.

This article is part of a Special Issue on DNA Nanotechnology

© 2016 Wiley-VCH Verlag GmbH & Co. KGaA, Weinheim

process, in which individual strands are cross-linked together by the complimentary domains. For instance, a 36-base three-domain OS strand can hybridize with up to three neighboring OS strands. The crosslinking among the individual OS strands leads to the formation of a three-domain OS hydrogel.

The multidomain one-strand design is easy to program to possess different numbers of domains and domain lengths, which are expected to affect the pore size and mechanical properties of OS hydrogels (Figure 1). We varied the number of domains from three to four, five, and six for the OS strands, while fixing the domain length (Figure 1 A). In addition, we designed and tested three-domain OS strands with different domain lengths of 12, 16, and 20 bases (Figure 1 B). When OS hydrogels were prepared at same weight concentrations, these changes resulted in different molecular concentrations, cross-link strengths (domain lengths), and numbers of connections between individual molecules (Figure 1 C). These changes, in turn, are expected to modulate the melting temperatures, mechanical properties, and pore sizes of OS hydrogels.

Characterization of OS hydrogels

OS hydrogels were prepared by using crude DNA strands in 20 mM of Tris·HCl buffer (pH 7.5) containing 10 mM of $MgCl_2$ without purification. To clearly verify the lengths of DNA strands, we purified the crude DNA strands by using 10% denaturing PAGE and extracted the major product bands. The purified DNA strands were then loaded into another 10% denaturing polyacrylamide gel, which revealed that all DNA strands exhibited the expected mobility (Figure 1 D). In a typical experiment for OS hydrogel assembly, an OS strand (e.g., OS-3-12) is dissolved in 30–100 μL buffer. At room temperature, the solution quickly forms a transparent gel within minutes (Figure 1 E). Raising the temperature above 70 °C disrupts the hybridization between DNA domains and changes the gel to liquid formation. Cooling the solution to room temperature again then brings it back to the gel formation. The liquid/gel switching process can be repeated multiple times without obvious changes in the speed of gel formation.

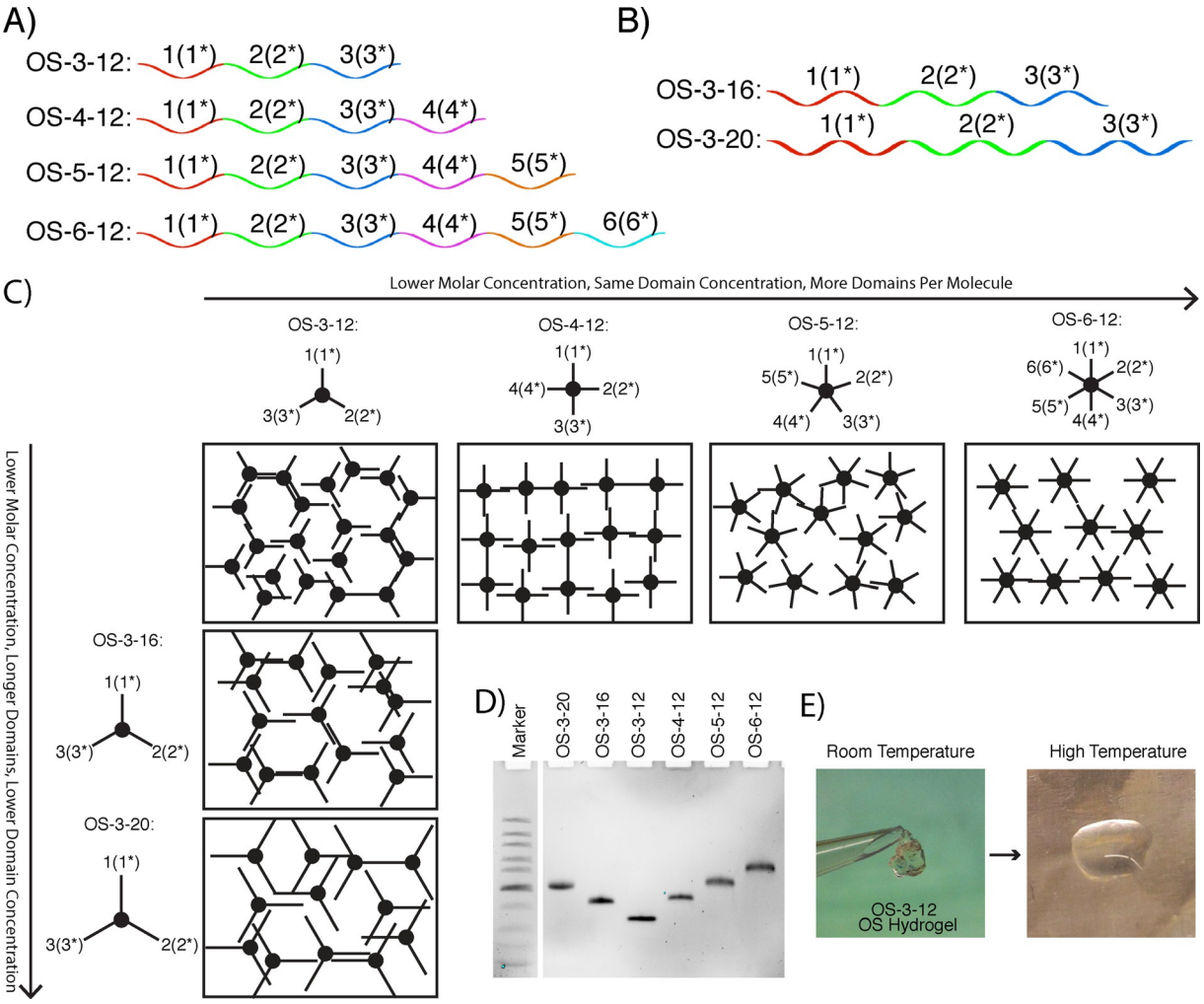

Figure 1. Designs and assembly of the multidomain OS hydrogels. A) OS strands with different numbers of palindromic domains. Each domain contains 12 bases. B) Three-domain OS strands with different domain lengths (16-base and 20-base). C) Domain changes are expected to affect the physical properties of OS hydrogels. D) 10% Denaturing PAGE analysis of purified OS strands. E) The OS-3-12 DNA hydrogel melts at high temperature (left) and reforms at room temperature (right).

© 2016 Wiley-VCH Verlag GmbH & Co. KGaA, Weinheim

The melting temperatures of OS hydrogel hybridization were directly related to the domain lengths. We measured the melting temperatures of strand hybridization by real-time PCR (Figure S1 and Table S1). The measurements were done on 2 μM concentrations of OS solutions, which remained in liquid form. Results revealed a correlation between domain length and hybridization temperature between the OS strands. OS-3-20, which has the longest domain length, exhibited the highest melting temperature at 70 °C, followed by OS-3-16 at 66 °C. In comparison, the number of domains showed little effect on melting temperature. OS-Y-12 (Y = 3, 4, 5, and 6) had melting temperatures between 58 and 61 °C.

Rheology measurements were performed at 25 °C to study how the physical properties of OS DNA hydrogels were affected by the domain lengths and number of domains per strand (Figure 2). First, we screened the storage modulus (G′) and loss storage (G″) of the DNA hydrogels with wt% concentrations varying from 0.2 to 3.0 wt% (Figure 2A). As expected, both G′ and G″ increased with increasing total DNA wt%. G′ was larger than G″ when the OS-3-12 concentration was higher than 0.5 wt%, indicating that OS-3-12 assembly above 0.5 wt% results in materials with more gel-like properties. The G′ of a 2 wt% OS-3-12 hydrogel was ~2800 Pa, slightly higher but comparable to that of a previously reported 2 wt% multistrand Y-motif/linker DNA hydrogel by Liu et al.[8a]

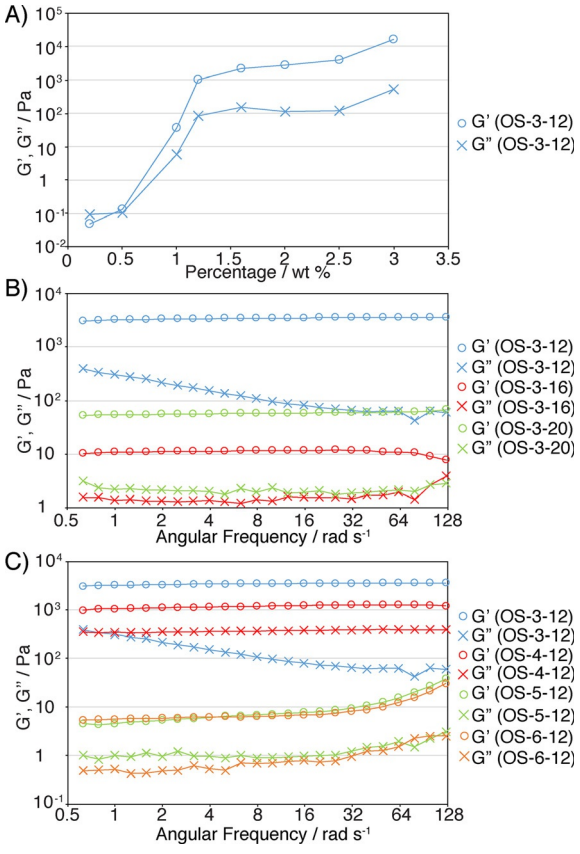

Figure 2. Rheological characterization of OS DNA hydrogels. A) Rheological measurement of the OS-3-12 DNA hydrogel with different weight percentages at a fixed 1 Hz frequency and a fixed 1% strain at 25 °C. B) Rheological angular frequency sweeps of 2 wt% OS hydrogels with different domain lengths. C) Rheological angular frequency sweeps of 2 wt% OS hydrogels with different numbers of domains. The angular frequency sweeps were performed at 1% strain at 25 °C.

At the same weight concentration, the physical properties of OS DNA hydrogels are affected by both the lengths of domains and the number of domains. We tested 12-base, 16-base, and 20-base three-domain OS DNA hydrogels at 2 wt% (Figure 2B). The results revealed that the rigidity of OS DNA hydrogels is inversely proportional to the domain lengths. Among the three samples, the OS-3-12 DNA hydrogel showed the strongest elastic behavior, whereas the OS-3-20 DNA hydrogel appeared softest. For three-domain OS DNA hydrogels at equal weight percentages, longer-domain OS DNA hydrogels have lower molar concentrations, which are expected to lead to lower levels of crosslinking among the DNA strand units. As a result, the longer domain and fewer crosslinks might be responsible for the softer DNA hydrogel formation.

The numbers of domains of OS strands also affect the DNA hydrogel properties. We performed rheology measurements on OS-3-12, OS-4-12, OS-5-12, and OS-6-12 DNA hydrogels at 2 wt% (Figure 2C). These hydrogels all utilize the 12-base domain design but with differing numbers of domains. Experimental results showed that OS DNA hydrogels with more domains exhibited lower rigidity. At the same weight concentration, the OS-3-12, OS-4-12, OS-5-12, and OS-6-12 DNA hydrogels should all have the same concentration of 12-base domains. However, the molar concentrations of these DNA hydrogels are inversely proportional to the number of domains of the OS strands. The relatively lower molar concentration of longer OS strands could lower the crosslinking efficiency, resulting in reduced hydrogel rigidity.

Two-strand multidomain hydrogels

The OS hydrogels can be easily modified to two-strand designs, which might be more desirable in certain applications (Figure 3). As an example, we demonstrated a three-domain, two-strand (TS) design by using nonpalindromic sequences (Figure 3A). The design includes two DNA strands: a TS-3-12-1 strand with three 12-base domains, each complementary to a 12-base domain on a TS-3-12-2 strand. As opposed to OS DNA hydrogels, a 2 wt% solution containing only one TS strand (TS-3-12-1 or TS-3-12-2) retained its liquid formation at room temperature (Figure 3B, left). On the other hand, transparent DNA hydrogel formed within minutes when equal amounts of 2 wt% TS-3-12-1 solution and 2 wt% TS-3-12-2 solution were mixed together at room temperature (Figure 3B, right). Therefore, the TS hydrogel system offers easy handling at room temperature while possessing the same programmability as the OS hydrogel system. The melting temperatures of 1 μM TS-3-12-1 and 1 μM TS-3-12-2 hybridization are both 58 °C, slightly lower than that of the 2 μM OS-3-12 strand. This is likely due to non-perfect stoichiometry between the two TS strands.

We compared 2 wt% TS-3-12 hydrogel with 2 wt% OS-3-12 hydrogel (Figure 3C). At 25 °C, the G′ values of OS and TS gels are both higher than their respective G″ values over the entire

© 2016 Wiley-VCH Verlag GmbH & Co. KGaA, Weinheim

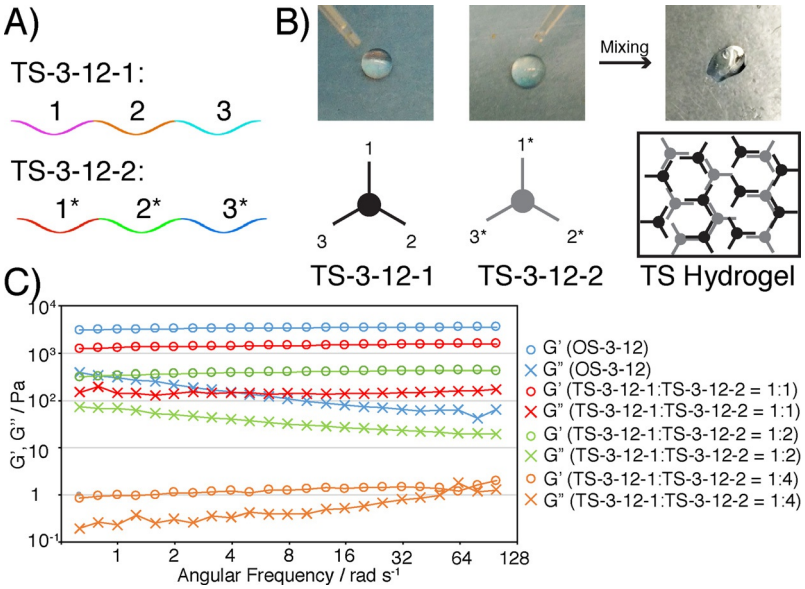

Figure 3. Two-strand (TS) hydrogels. A) The TS-3-12-1 strand contains three 12-base domains complementary to the three 12-base domains on the TS-3-12-2 strand. B) Solutions of TS-3-12-1 and TS-3-12-2 (left) only formed hydrogels when the two solutions were mixed together at room temperature (right). C) Rheological angular frequency sweeps of 2 wt% OS-3-12 and 2 wt% TS-3-12 DNA hydrogels. The angular frequency sweeps were performed at 1% strain at 25 °C.

exchange range, a typical mechanical property of hydrogels. However, the TS-3-12 DNA hydrogel showed lower G′ and G″ values than OS-3-12. In addition, the gap between the G′ and G″ values of TS-3-12 is narrower than the G′/G″ gap for OS-3-12. These results suggest that the OS DNA hydrogels exhibit more rigidity than TS DNA hydrogels of the same concentration. The lower rigidity of TS DNA hydrogels might be partially due to the imperfect stoichiometry between the two TS DNA strands.

We then tested the mechanical properties of 2 wt% TS hydrogels with different ratios between TS-3-12-1 and TS-3-12-2 (Figure 3C). When the TS-3-12-1 to TS-3-12-2 ratio was changed from 1:1 to 1:2 and 1:4, we observed significantly reduced stiffness, especially at the 1:4 ratio, likely due to relatively larger numbers of unhybridized single-stranded domains. At the 1:4 ratio, the G′ value of the TS-3-12 gel dropped to the low value of ~1 Pa. This result is consistent with the previous study of the Y-motif/linker hydrogel.[8a] Liu et al showed that at ratios of 2:1 and 1:3, the Y-motif/linker gel had low a G′ value, around 0.1 Pa, likely also due to the large excess of unbonded motifs.

Cargo loading and releasing

Multidomain OS DNA hydrogels provide a simple system for carrying single-component or multi-component cargos. We demonstrated cargo loading and release by using the OS-6-12 hydrogel (Figure 4). First, we demonstrated quick release of small molecule cargos. Bromophenol Blue was loaded onto a 30 μL 2 wt% hydrogel, then the hydrogel was immersed in 60 μL buffer (Figure 1A). Because Bromophenol Blue is much smaller then the expected pore size of the hydrogel, the Bromophenol Blue quickly diffused to the buffer, whereas the DNA hydrogel volume remained unchanged over 4 h. Unlike small-sized molecules, large cargo can be trapped inside the DNA hydrogel for a long period of time. We prepared a 50 μL 2 wt% DNA hydrogel with 10 nm gold nanoparticles and then added 100 μL buffer on top of the red-colored hydrogel (Figure 1B). Over a period of 96 h, no obvious release of gold nanoparticles was observed. It is worth noting that the hydrogel started to expand and broke apart after 4 h. This is likely due to the solution exchange between the buffer and hydrogel loaded with gold nanoparticles.

We then demonstrated that the domains of the OS-6-12 strand can be modified for specific binding and releasing of DNA strands (Figure 4C and D). Unlike physically trapping cargos during DNA hydrogel formation, the hybridization-loaded DNA cargos can be engineered for release in response to specific stimuli, such as complementary DNA strands. The modified strand was named (Cy5)-OS-6-12. The Cy5-DNA binds to (Cy5)-OS-6-12 during hydrogel formation (Figure 4C). The other five active palindromic domains crosslink (Cy5)-OS-6-12 to form a hydrogel. During the release step, DNA strand (Cy5)-Release, complementary to both the poly-T segment and the first domain, was added to replace the Cy5-DNA. We added the Cy5-DNA strand to (Cy5)-OS-6-12 at a 1:7 molar ratio to form a DNA hydrogel and studied Cy5-DNA release over 96 h (Figure 4D). The 30 μL 2 wt% hydrogel, submerged in 100 μL buffer, retained its volume and shape during the study. An excessive amount of (Cy5)-Release strand was added at hour 0. A gradual release of Cy5-DNA was observed and completed after 96 h. In contrast, no release was observed in the absence of (Cy5)-Release strand under the same conditions (Figure 4E).

The OS-6-12 strand was modified to further demonstrate loading of multiple DNA strands with controlled stoichiometry (Figure 4F, G). In the modified strand design, the first and last

© 2016 Wiley-VCH Verlag GmbH & Co. KGaA, Weinheim

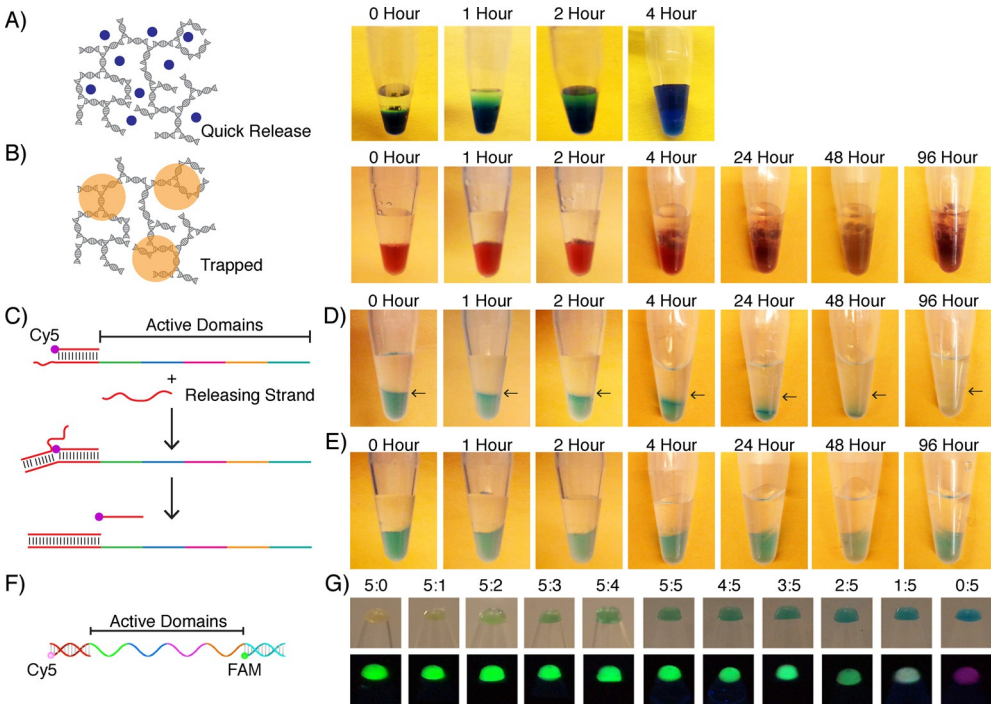

Figure 4. Loading cargo molecules by using OS-6-12 DNA hydrogels. A) Loading and quick releasing of Bromophenol Blue. B) Loading of 10 nm gold nanoparticles in OS-6-12 hydrogel. Particles were trapped and could not be released after 96 h incubation in buffer. C) Design of loading and releasing of the Cy5-DNA. Releasing was achieved by using a strand displacement reaction. D) The Cy5-DNA was fully released after 96 h, whereas the hydrogel retained its original shape. Black arrows indicate the top edge of the hydrogel. E) No Cy5-DNA release in the absence of the releasing DNA strand. F) Two domains of OS-6-12 were modified to bind to the Cy5-DNA strands and FAM-DNA, respectively. G) White-light images and UV images of FOS-6-12 DNA hydrogels with the two fluorescence dyes at different loading ratios from 5:0 to 0:5.

domains of OS-6-12 were changed to nonpalindromic sequences to hybridize with the Cy5-DNA and a FAM-labeled DNA (FAM-DNA), respectively (Figure 4F). The modified strand ((Cy5/FAM)-OS-6-12) has four remaining palindromic domains available for crosslinking. We mixed the two fluorophore-labeled DNA strands with OS-6-12 at a 1:7 ([Cy5-DNA + FAM-DNA]:[(Cy5/FAM)-OS-6-12]) molar ratio to form a DNA hydrogel loaded with two fluorophores. The ratio between the FAM-DNA and Cy5-DNA strands was varied from 5:0 to 0:5, resulting in a series of DNA hydrogels of different colors (Figure 4G).

Conclusions

In summary, we have demonstrated a group of low-cost, programmable DNA hydrogels by using a simple one-strand multipalindromic domain design. By modifying the domain length and number of domains, we programmed the OS DNA hydrogels to exhibit variable chemical and physical characteristics, such as melting temperature and rheological properties. In addition, the domains of OS DNA hydrogels can be easily modified for loading molecular cargos, whereas the unmodified palindromic domains are still capable of crosslinking with each other to form hydrogels. We also showed that the multidomain design could be implemented to make multistrand nonpalindromic-sequence DNA hydrogels. By applying our new design strategy to longer DNA strands and/or more DNA strands, we believe increasingly complex and programmable DNA hydrogels can be readily constructed. We expect these new DNA hydrogels will provide a low-cost, highly programmable platform for many potential biological and biomedical applications.

Experimental Section

Materials: All oligonucleotides were either synthesized on an Expedite 8900 Nucleic Acid Synthesis system or purchased from IDT. The synthesis and deprotection processes were carried out according to the instructions provided by the reagent manufacturers. Subsequently, the deprotected DNA was precipitated by adding $^{1}/_{10}$ volume of 3 M NaOAc (pH 5.2) and 3× volume of cold EtOH. After placing in a freezer at −20 °C for 30 min, the DNA products were collected by centrifugation at 22000 *g* for 30 min. DNA products were further purified by 10% denaturing PAGE. Two fluorophore-labeled DNA were purchased from IDT. Gold nanoparticles (10 nm) were purchased from BBI Solutions. All chemicals were of reagent grade or higher, and were used as received.

DNA sequences

OS-3-12: AACGT TAACG TTTGG GAATT CCCAA TCGAC GTCGA T

OS-4-12: AACGT TAACG TTTGG GAATT CCCAA TCGAC GTCGA TCGTG GATCC ACG

OS-5-12: AACGT TAACG TTTGG GAATT CCCAA TCGAC GTCGA TCGTG GATCC ACGGA GGCGC GCCTC

© 2016 Wiley-VCH Verlag GmbH & Co. KGaA, Weinheim

OS-6-12: AACGT TAACG TTTGG GAATT CCCAA TCGAC GTCGA TCGTG GATCC ACGGA GGCGC GCCTC AGCGG TACCG CT

OS-3-16: ACAAC GTTAA CGTTG TAGTG GGAAT TCCCA CTTAA TCGAC GTCGA TTA

OS-3-20: ATACA ACGTT AACGT TGTAT TTAGT GGGAA TTCCC ACTAA AATAA TCGAC GTCGA TTATT

TS-3-12-1: TATCA GATTC GATGC AAGTG AAATG TCGGT AACCA G

TS-3-12-2: TCGAA TCTGA TAATT TCACT TGCAC TGGTT ACCGA C

(Cy5/FAM)-OS-6-12: TGTGT GTGTG TGTTG GGAAT TCCCA ATCGA CGTCG ATCGT GGATC CACGG AGGCG CGCCT CTCCT TCCTT CCTT

(Cy5)-OS-6-12: TTTTT TTTTG TGTGT GTGTG TTGGG AATTC CCAAT CGACG TCGAT CGTGG ATCCA CGGAG GCGCG CCTCA GCGGT ACCGC T

(Cy5)-Release: ACACA CACAC ACAAA AAAAA A

Cy5-DNA: ACACA CACAC ACA-Cy5

FAM-DNA: AAGGA AGGAA GGA-FAM

DNA hydrogel preparation

OS DNA hydrogels: DNA strands were dissolved in a buffer solution containing Tris·HCl buffer (20 mM, pH 7.5) and $MgCl_2$ (10 mM) to obtain the final desired concentration, followed by heating to 95 °C for 5 min and cooling at room temperature for 2 h to form the final OS DNA hydrogels.

OS-3-12 DNA was observed to dissolve into clear aqueous solution after less than 1 min of heating at about 55–60 °C. Following removal from heat, the gel reformed after cooling to room temperature. The liquid/gel switching process could be repeated multiple times without an obvious change in gel formation speed.

TS DNA hydrogels: TS-3-12-1 and TS-3-12-2 were dissolved in a buffer solution containing Tris·HCl buffer (20 mM, pH 7.5) and $MgCl_2$ (10 mM) to obtain the final desired concentrations. The two solutions were then mixed together in a 1:1 ratio and then subjected to a 2 h annealing process (from 95°C to room temperature) to form the TS DNA hydrogels.

Measurements of melting temperature: Melting points were measured on a Step One Plus real-time PCR system (Applied Biosystems). All DNA strands were dissolved with Tris·HCl buffer (20 mM, pH 7.5) containing $MgCl_2$ (10 mM) to reach final concentrations of 2 μM. SYBR Green was added as the fluorescence source. All samples were heated to 95 °C for 30 seconds, followed by cooling to 25 °C. The temperature was then increased to 85 °C with a speed of 0.3 °C per step.

Rheology measurements: Rheological tests were carried out on an AR2000ex rheometer equipped with a temperature controller. Frequency sweep tests were carried out on mixtures between 0.64 and 64 rad s^{-1} at 25 °C at a fixed strain of 1%. Rheological experiments were performed on 25 mm parallel plates with 20 μL of hydrogels (resulting in a gap size of 0.05 mm), and an angular frequency sweep (0.64–64 rad s^{-1}) was carried out with a fixed strain sweep of 1% at 25 °C.

Cargo loading and releasing: Bromophenol-blue- and gold-nanoparticle-loaded hydrogels: 1% Bromophenol Blue (1 μL) was added to 2 wt% OS-6-12 hydrogel (30 μL), heated to 95 °C, mixed with a vortex mixer, then allowed to cool to room temperature. Gold nanoparticle solution (10 nm) was concentrated to 400 nM by centrifugation (12000 *g*, 10 min) before being added to the DNA hydrogels. Concentrated 10 nm gold nanoparticle solution (2 μL, 400 nM) was added to 2 wt% OS-6-12 hydrogel (30 μL), heated to 95 °C, mixed with a vortex mixer, and then allowed to cool to room temperature.

Cy5-DNA hydrogel and release: Cy5-DNA solution (100 μM) containing Tris·HCl buffer (20 mM, pH 7.5) and $MgCl_2$ (10 mM) were added to 2 wt% (Cy5)-OS-6-12 hydrogel (30 μL), followed by heating to 95 °C for 5 min and cooling at room temperature for 2 h to form the DNA hydrogels. The final ratio of (Cy5)-OS-6-12:Cy5-DNA was around 7:1. Tris buffer (100 μL) containing (Cy5)-Release DNA (300 μM) was added for the strand-displacement study.

Cy5- and FAM-DNA hydrogels: Variable amounts of 100 μM FAM-DNA and 100 μM Cy5-DNA solution containing Tris·HCl buffer (20 mM, pH 7.5) and of $MgCl_2$ (10 mM) were added to 10 μL 2 wt% (Cy5)-OS-6-12 or (Cy5/FAM)-OS-6-12 hydrogel, followed by heating to 95 °C for 5 min and cooling at room temperature for 2 h to form the final DNA hydrogels. The final ratio of (Cy5/FAM)-OS-6-12:(FAM-DNA + Cy5-DNA) was 7:1.

Acknowledgements

This work was supported by a Wallace H. Coulter Department of Biomedical Engineering Faculty Startup Grant and a Winship Cancer Institute Billi and Bernie Marcus Research Award to Y.K., and National Science Foundation (NSF) grants CMMI1250199 and CMMI1250235 to E.R.W.

Keywords: DNA nanotechnology · hydrogel · programmable nanomaterials

[1] a) E. M. Ahmed, *J. Adv. Res.* **2015**, *6*, 105–121; b) J. Elisseeff, *Nat. Mater.* **2008**, *7*, 271–273.

[2] a) H. Jung, J. S. Park, J. Yeom, N. Selvapalam, K. M. Park, K. Oh, J.-A. Yang, K. H. Park, S. K. Hahn, K. Kim, *Biomacromolecules* **2014**, *15*, 707–714; b) C. Merceron, S. Portron, M. Masson, B. H. Fellah, O. Gauthier, J. Lesoeur, Y. Cherel, P. Weiss, J. Guicheux, C. Vinatier, *Bio-Med. Mater. Eng.* **2010**, *20*, 159–166; c) D. Kumar, I. Gerges, M. Tamplenizza, C. Lenardi, N. R. Forsyth, Y. Liu, *Acta Biomater.* **2014**, *10*, 3463–3474.

[3] a) T. R. Hoare, D. S. Kohane, *Polymer* **2008**, *49*, 1993–2007; b) A. Vashist, A. Vashist, Y. K. Gupta, S. Ahmad, *J. Mater. Chem. B* **2014**, *2*, 147–166.

[4] E. Cambria, K. Renggli, C. C. Ahrens, C. D. Cook, C. Kroll, A. T. Krueger, B. Imperiali, L. G. Griffith, *Biomacromolecules* **2015**, *16*, 2316–2326.

[5] J. Song, K. Im, S. Hwang, J. Hur, J. Nam, G. O. Ahn, S. Hwang, S. Kim, N. Park, *Nanoscale* **2015**, *7*, 9433–9437.

[6] a) N. C. Seeman, *Nature* **2003**, *421*, 427–431; b) P. W. K. Rothemund, *Nature* **2006**, *440*, 297–302; c) S. D. Perrault, W. M. Shih, *ACS Nano* **2014**, *8*, 5132–5140; d) J. Mikkilä, A.-P. Eskelinen, E. H. Niemelä, V. Linko, M. J. Frilander, P. Törmä, M. A. Kostiainen, *Nano Lett.* **2014**, *14*, 2196–2200; e) L. Liang, J. Li, Q. Li, Q. Huang, J. Shi, H. Yan, C. Fan, *Angew. Chem. Int. Ed.* **2014**, *53*, 7745–7750; *Angew. Chem.* **2014**, *126*, 7879–7884; f) M. Langecker, V. A. List, J. List, F. C. Simmel, *Acc. Chem. Res.* **2014**, *47*, 1807–1815; g) N. Chen, J. Li, H. Song, J. Chao, Q. Huang, C. Fan, *Acc. Chem. Res.* **2014**, *47*, 1720–1730; h) Z.-G. Wang, C. Song, B. Ding, *Small* **2013**, *9*, 2210–2222; i) J. R. Burns, E. Stulz, S. Howorka, *Nano Lett.* **2013**, *13*, 2351–2356; j) Y. Kamiya, H. Asanuma, *Acc. Chem. Res.* **2014**, *47*, 1663–1672; k) D. Yuan, X. Du, J. Shi, N. Zhou, J. Zhou, B. Xu, *Angew. Chem. Int. Ed.* **2015**, *54*, 5705–5708; *Angew. Chem.* **2015**, *127*, 5797–5800.

[7] a) Y. Li, Y. D. Tseng, S. Y. Kwon, L. d'Espaux, J. S. Bunch, P. L. McEuen, D. Luo, *Nat. Mater.* **2004**, *3*, 38–42; b) S. H. Um, J. B. Lee, N. Park, S. Y. Kwon, C. C. Umbach, D. Luo, *Nat. Mater.* **2006**, *5*, 797–801; c) E. Cheng, Y. Xing, P. Chen, Y. Yang, Y. Sun, D. Zhou, L. Xu, Q. Fan, D. Liu, *Angew. Chem. Int. Ed.* **2009**, *48*, 7660–7663; *Angew. Chem.* **2009**, *121*, 7796–7799; d) J. B. Lee, S. Peng, D. Yang, Y. H. Roh, H. Funabashi, N. Park, E. J. Rice, L. Chen, R. Long, M. Wu, D. Luo, *Nat. Nanotechnol.* **2012**, *7*, 816–820.

© 2016 Wiley-VCH Verlag GmbH & Co. KGaA, Weinheim

[8] a) Y. Xing, E. Cheng, Y. Yang, P. Chen, T. Zhang, Y. Sun, Z. Yang, D. Liu, *Adv. Mater.* **2011**, *23*, 1117 – 1121; b) C. Li, P. Chen, Y. Shao, X. Zhou, Y. Wu, Z. Yang, Z. Li, T. Weil, D. Liu, *Small* **2015**, *11*, 1138 – 1143; c) C. Li, A. Faulkner-Jones, A. R. Dun, J. Jin, P. Chen, Y. Xing, Z. Yang, Z. Li, W. Shu, D. Liu, R. R. Duncan, *Angew. Chem. Int. Ed.* **2015**, *54*, 3957 – 3961; *Angew. Chem.* **2015**, *127*, 4029 – 4033; d) J. Li, C. Zheng, S. Cansiz, C. Wu, J. Xu, C. Cui, Y. Liu, W. Hou, Y. Wang, L. Zhang, I. T. Teng, H. H. Yang, W. Tan, *J. Am. Chem. Soc.* **2015**, *137*, 1412 – 1415.

Manuscript received: December 22, 2015
Accepted article published: February 17, 2016
Final article published: March 21, 2016

© 2016 Wiley-VCH Verlag GmbH & Co. KGaA, Weinheim